ACTA TECHNICA CORVINIENSIS – Bulletin of Engineering | e–ISSN: 2067 – 3809
Tome XVIII [2025] | Fascicule 2 [April – June]

[1.] László Péter KISS, [2.] M. H. DAUD

ON THE MECHANICAL STATE OF ARCHES AT BUCKLING CONDITION

[1.]Institute of Applied Mechanics, University of Miskolc, 3515 Miskolc–Egyetemváros, HUNGARY
[2.]University of Miskolc, 3515 Miskolc–Egyetemváros, HUNGARY

Abstract: The in–plane stability and mechanical state of pinned–fixed arches under an arbitrarily positioned concentrated radial load is assessed. By assumption, the cross–sections rotate as rigid bodies and stay perpendicular to the centerline. The beam model applied is non–linear through the rotations and is based on the single layer Euler–Bernoulli hypothesis. The material is linearly elastic, isotropic and does not vary along the centerline. Graphical results are given for the lowest buckling loads in terms of the geometry and load position. Furthermore, the typical normal and tangential displacements together with the bending moment, shear force and axial force distributions are assessed too.
Keywords: arch, stability, non–linear, displacements, inner forces

INTRODUCTION

Arches are preferred elements that can be used in several engineering structures. One preferred application is in lightweight roof structures.

There is a vast amount of literature available on the buckling of beams and arches. For a comprehensive summary, we refer to books [1,2]. Early arch models, such as [3], assumed the inextensibility of the centroidal axis. However, it was later proved [4,5] that this simplification could overestimate the maximum allowable load, making earlier models outdated.

In recent decades, there has been significant progress in addressing various shallow arch problems, with numerous articles published on the topic – see, example [6,7,8,9,10]. These studies primarily focus on in–plane stability and employ a range of approaches and assumptions. Some provide solutions for homogeneous or functionally graded members, while others consider different load types, such as concentrated or distributed loads along the centroidal axis. The cross–sectional geometry is both constant throughout the entire arch, or varies in segments, and there are various support configurations considered in these studies.

Article [11] thoroughly investigated the in–plane linear elastic buckling of arches. With respect to the in–plane nonlinear buckling, papers [12,13] addressed the in–plane nonlinear elastic buckling and post–buckling of circular shallow arches, taking into account the pre–buckling deformation effect, and came up with exact analytical solutions.

Based on these former works, here we present a non–linear model capable of dealing with circular arches. There are two aims. First, to find the lowest buckling loads when there is an external force in radial direction at an arbitrary position. Secondly and more importantly, to investigate how the tangential– and normal displacements, bending moments, shear forces and axial forces change just prior to buckling as the load position is varied.

The text of this paper is composed of five sections. Following this introduction, the major properties of the mechanical model are given. Then, in Section 3, the computational results are provided graphically. The Conclusions section gathers the most important findings, and finally, the list of References close the article.

MODEL PROPERTIES

The mechanical model is the same as detailed in [14, 15]. Figure 1 shows the centerline of the circular arch. The pinned–fixed arch, whose initial constant radius is ρ_o, is loaded by a concentrated radial force P_ζ.

The load position is arbitrary, and is identified by the angle coordinate $\varphi=a$ – its sign matters because of the uneven supports and its magnitude is not greater than the semi–vertex angle ϑ.

The membrane strain on the centerline is approximated as

$$\varepsilon_m = \frac{du_0}{ds} + \frac{w_0}{\rho_0} + \frac{1}{2}\left(-\frac{dw_0}{ds}\right)^2 \quad (1)$$

where u_0 and w_0 are the axial and radial displacements and $s=\rho_0\varphi$ is the arc coordinate. The arc coordinate is zero at the crown of the arch.

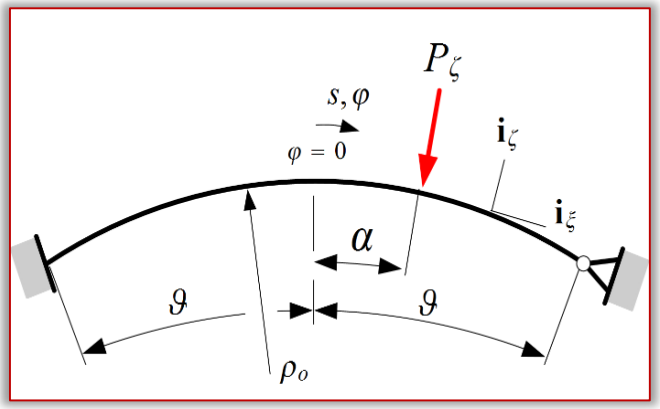

Figure 1. The one–dimensional pinned–fixed beam model with the loading

The axial force and the bending moment are defined as

$$N = A\varepsilon_m - \frac{IE}{\rho_0}\left(\frac{du_0}{\rho_0 ds} - \frac{d^2w_0}{ds^2}\right), \quad (2)$$

$$M = -IE\left(\frac{d^2w_0}{d^2s} + \frac{w_0}{{\rho_0}^2}\right) \quad (3)$$

with IE being the bending stiffness and A is the cross–sectional area. The static equilibrium equations for arches with uniform cross–section and radial load are simply

$$\varepsilon_m{}' = 0, \quad (4a)$$

$$W''' + (\mu^2 + 1)W'' + \mu^2 W = \mu^2 - 1, \quad (4b)$$

given the notational convention

$$\frac{d()}{ds} = ()' \quad (5)$$

and the parameters

$$\mu^2 = 1 - m\varepsilon_m \ , \ m = \frac{A{\rho_0}^2}{I} \ . \quad (6)$$

Furthermore, $W=w_0/\rho_0$ is a dimensionless radial displacement. Former equations (4a), (4b) together with the boundary conditions valid for pinned–fixed arches define a boundary value problem that was solved to get the lowest buckling loads and related strains of arches under an arbitrary concentrated radial load.

RESULTS

Evaluation of the model is presented hereinafter Computations were carried out using mathematical software Maple. During our efforts, the quotient of the arch length $S=2\rho_o\vartheta$ and the r radius of gyration

$$r^2 = I/A \quad (7)$$

and the some previously introduced parameters, like m, a/ϑ; ϑ are used. Furthermore,

$$P = \frac{P_\zeta \rho_0^2 \vartheta}{2IE} \quad (8)$$

is a dimensionless critical load.

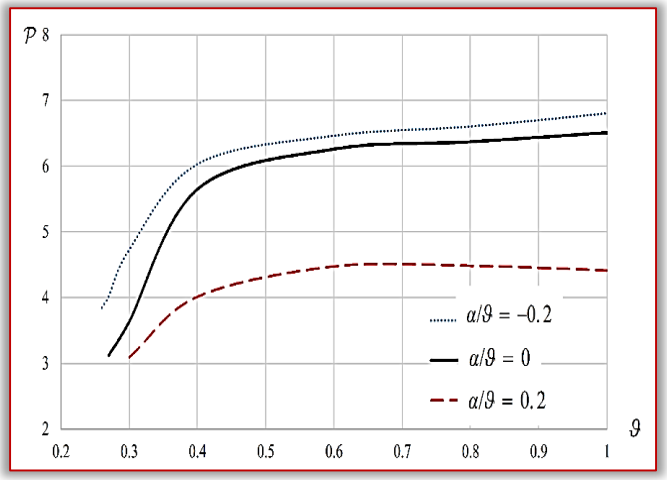

Figure 2. Lowest dimensionless buckling loads for S/r = 80

In Figure 2 it is shown how the lowest dimensionless buckling load varies with the semi–vertex angle of the arch when the S/r ratio is 80. Three load positions are assessed: $a/\vartheta=[-0.2;0;0.2]$. Because the supports are unsymmetrical, the sign of the load position is relevant in terms of the load bearing abilities. The continuous curve represents that the load is in the mid–span. It shows a monotonous trend. For very small angles, there is no buckling expected.

After that the critical load increases steeply until about $\vartheta\approx0.4$. Later, it flattens and actually the arch angle does not have so drastic effects as beforehand. When the load position parameter is set to –0.2 (the load application point is moved closer to the fixed support), the critical loads exceed the former case throughout.

The greatest improvement is experienced at $\vartheta\approx0.27$ with +28.8%, while in the vicinity of $\vartheta\approx0.7$,

the relative difference is the lowest, staying below 5%. However, when the load is moved closer to the pinned support as a/ϑ=+0.2, the critical load values are much lower. The range in which it changes in relation to the crown–point load is within –14.9...–32.2%, having the greatest discrepancy at ϑ=1.

In the following, some field distributions are presented along the arch centerline, using the dimensionless coordinate φ/ϑ ∈[−1;1]. The selected arch for the demonstrations have the following properties. It has a homogeneous, rectangular cross–section with A=8 mm^2 and I=2.66 mm^4. The modulus of elasticity E is 200 GPa. Let us use m=10^5 so that ρ_o=182.5 mm and ϑ=0.25. The effect of four load positions are assessed when the related buckling load is applied. This buckling load is different for each case – see Figure 2.

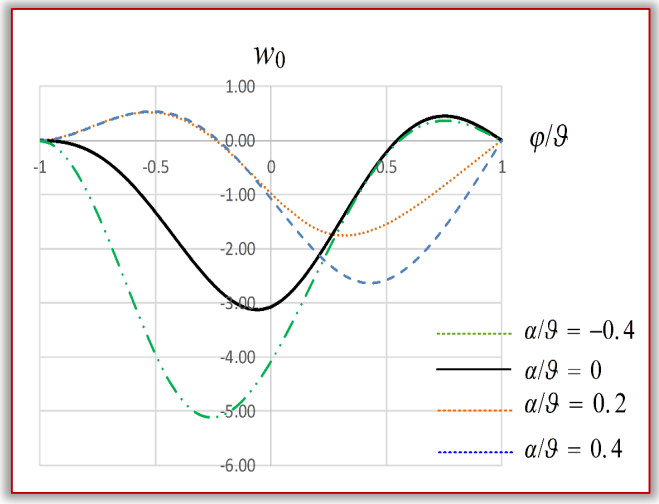

Figure 3. The normal displacements in [mm] along the centerline

The radial displacement field is given in Figure 3. The lowest displacements occur at the moment of buckling when a/ϑ = 0.2, and the greatest ones at a/ϑ=–0.4. This later case holds the greatest buckling load at the same time. Because of the unsymmetrical supports, even the displacement pattern at a=0 is not symmetric.

When we move on to the tangential displacements, as per Figure 4, it can be concluded that these values are much lower than the radial displacements. It is due to the fact that the selected arch is shallow. Here, there is much less relative difference in the peak values, in comparison to the radial displacements.

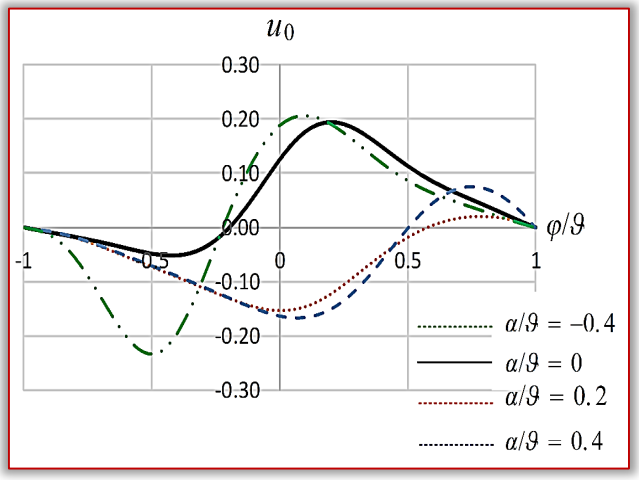

Figure 4. The tangential displacements in [mm] along the centerline

Proceeding with the bending moment distribution (Figure 5), it turns out that arches when a/ϑ = −0.4 can bear by far the highest levels until buckling and the lowest values are found throughout the centerline if a/ϑ = 0.2. The difference between the peak values is more than 2.5 times, that is quite substantial. It is also clearly visible that at the right pinned support, the bending moment is always zero, while the left–sided fixed support can bear moment load.

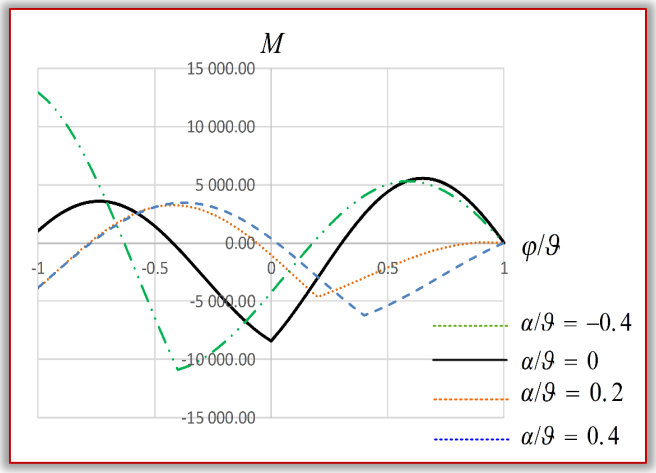

Figure 5. The bending moments in [Nmm] along the centreline

The shear force distribution is shown in Figure 6. It always has a discontinuity, exactly at the external load position. From these graphs, the buckling load values can also be read, which the discontinuity itself is.

As shown in Figure 7, the axial force is almost evenly distributed for each case, although, the load position clearly affects the actual values. The maximum values on account of the load position are about 1.6 times of the minimum. Greatest values are found for crown–point load. Overall, it can be concluded that displacing the load from the crown in both directions

makes the axial force decrease at the moment of buckling.

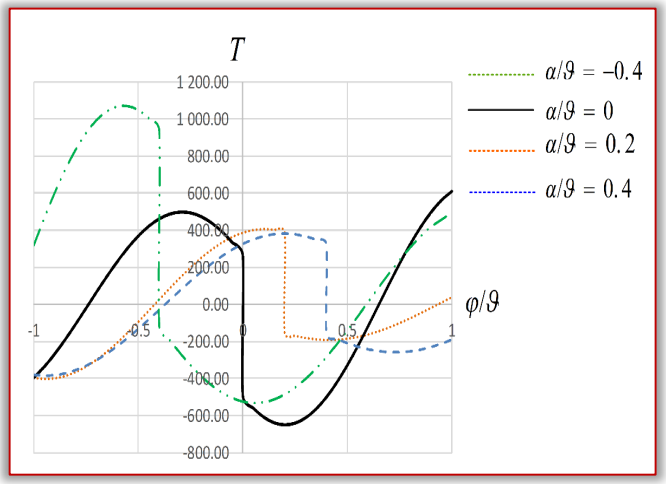

Figure 6. The shear force in [N] along the centerline

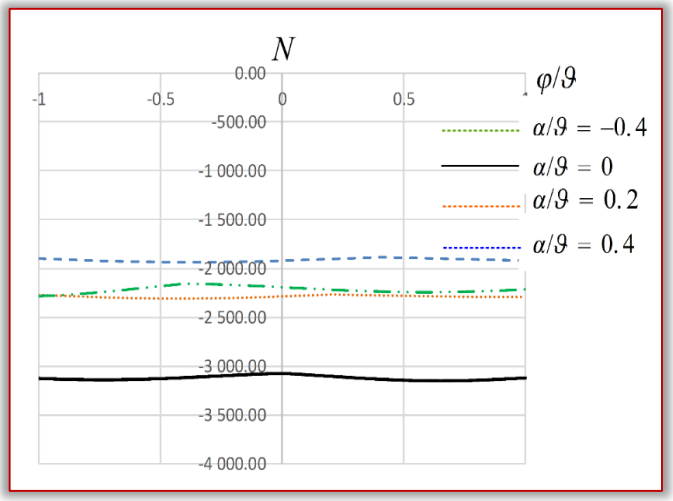

Figure 7. The axial force in [N] along the centerline

The relative values are given in the forthcoming figures (Figures 8–12) regarding the previous fields. The actual values are always divided by the maximum for mid–span load along the vertical coordinate axis. In this way, it is easier to make comparisons between the results of the various loading positions.

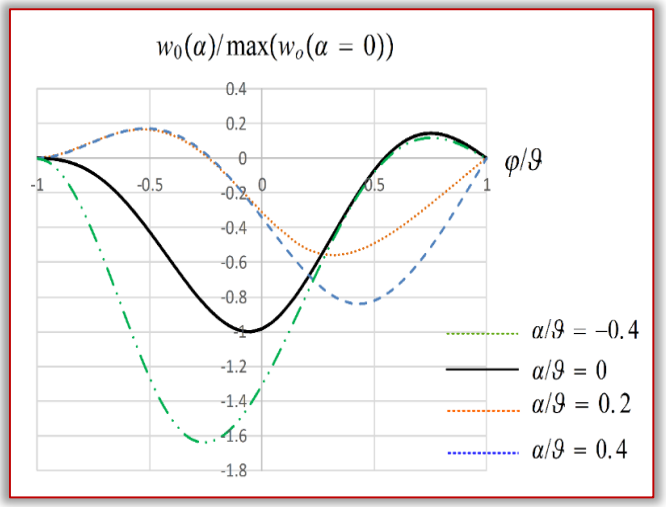

Figure 8. The relative radial displacement along the centerline

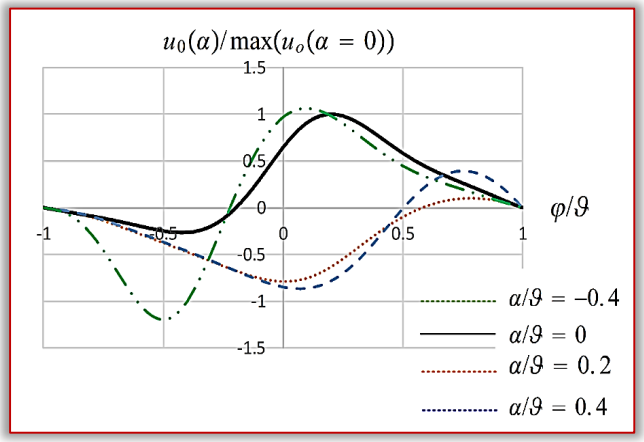

Figure 9. The relative tangential displacement along the centerline

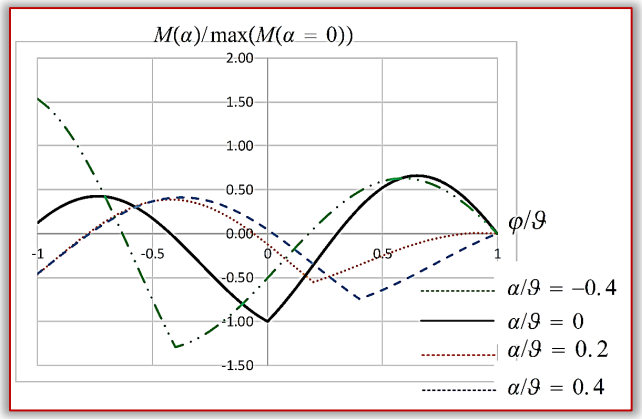

Figure 10. The relative bending moment along the centerline

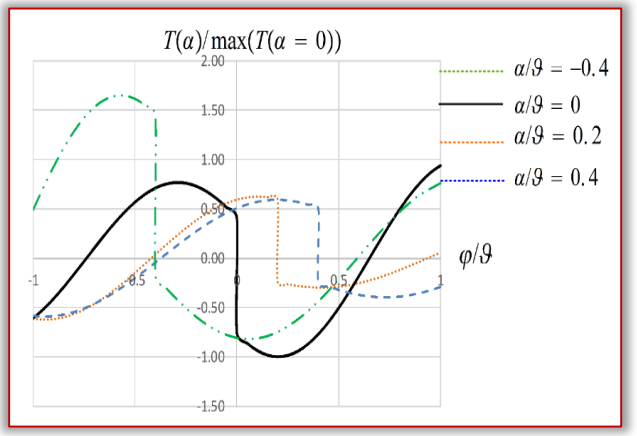

Figure 11. The relative shear force along the centreline

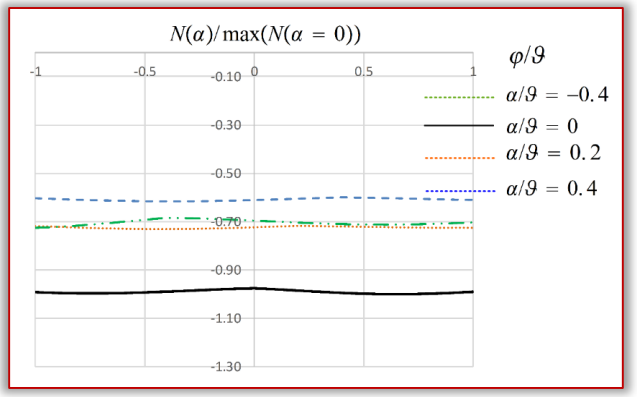

Figure 12. The relative axial force along the centerline

CONCLUSIONS

The topic of the article is the stability pinned–fixed circular arches. The problem solved is physically linear and geometrically nonlinear. The introduced one–dimensional beam model is based on the single–layer Euler–Bernoulli hypothesis.

The lowest buckling loads are evaluated. Furthermore, at the moment of buckling, the typical fields are plotted along the centerline for comparisons. It is found that the load position has significant effects not only on the buckling load but also on the typical values and patterns of the displacements and inner forces.

References

[1] Bazant, Z., Cedolin, L.: Stability of Structures. World Scientific, 2010.
[2] Dym, C. L.: Stability Theory and Its Applications to Structural Mechanics. Dover, 2002.
[3] Hurlbrink, E.: Berechnung von Rohrenartigen Kärpern, die Unter Ausserem Drucke Stehen. Schiffbau, 9(14):517–523, 1907–1908.
[4] Timoshenko, S. P., Gere, J. M.: Theory of elastic stability. New York, McGraw–Hill, 1961.
[5] Schreyer, H. L., Masur, E. F.: Buckling of shallow arches. Journal of Engineering. Mechanics Division ASCE, 92:1–17, 1966
[6] Bradford, M. A., Pi, Y.–L., Tin–Loi, F.: Non–linear in–plane buckling of rotationally restrained shallow arches under a central concentrated load. International Journal of Non–Linear Mechanics, 43:1–17, 2008
[7] Babaei, H., Kiani, Y., Eslami, M. R.: Thermomechanical nonlinear in–plane analysis of fix–ended FGM shallow arches on nonlinear elastic foundation using two–step perturbation technique. International Journal of Mechanics and Materials in Design, 15:225–244, 2019.
[8] Yan, S.–t., Shen, X., Chen, Z., Jin, Z.: Collapse behavior of non–uniform shallow arches under a concentrated load for fixed and pinned boundary conditions. International Journal of Mechanical Sciences, 137:46 – 67, 2018.
[9] Yan, S.–t., Shen, X., Chen, Z., Jin, Z.: On buckling of non–uniform shallow arch under a central concentrated load. International Journal of Mechanical Sciences, 133:330 – 343, 2017.
[10] Adam, C., Ladurner, D., Furtmüller, T.: In–plane buckling of flexibly bonded three–layer pinned–fixed half–sine shallow arches, International Journal of Non–Linear Mechanics, 151:104369, 2023.
[11] Simitses, G. J.: An introduction to the elastic stability of structures, Journal of Applied Mechanics, 43(2), 383–384, 1976.
[12] Bradford, M. A., Uy, B., Pi ,Y.–L.: In–plane elastic stability of arches under a central concentrated load, Journal of Engineering Mechanics, ASCE, 128(7), 710, 2002.
[13] Pi, Y.–L., Bradford, M. A., Uy, B.: In–plane stability of arches, International Journal of Solids and Structures, 39, 105–125, 2002.
[14] Abderrazek, M., Kiss, L. P., Murawski, K. The influence of non–symmetrical supports on the stability of arches. GÉP, 15(3–4):69–72., 2024.
[15] Kiss, L. P., Jalalova, P., Mehdiyev, Z.: Deformations and internal forces in arches under a concentrated force, Journal of Mechanics of Materials and Structures, 18(4):551–565, 2023.

ISSN: 2067–3809